

PRE-AMPLIFIER IMPEDANCE MATCHING FOR CRYOGENIC BPMs

P. Kowina, M. Freimuth, K. Gütlich, W. Kaufmann, H. Rödl, J. Wiessmann, GSI, Darmstadt, Germany
 N. Sobel, F. Völklein, RheinMain University of Applied Sciences, Wiesbaden, Germany

Abstract

Beam Position Monitors (BPMs) for the FAIR superconducting synchrotron SIS100 [1] will be installed inside the cryostats of quadrupole magnets. This contribution focuses on the coupling path between BPM electrodes and low noise amplifiers installed outside the cryostat. Matching transformers (MT) meet well the requirements of reflection-free signal transfer through the relative long cable without loading the capacitive BPM by 50 Ω. Transformers based on toroidal cores made out of nanocrystalline Vitroperm-500F were tested. The form of windings and circuit geometry were optimized to improve linearity and allow for resonance-free transmission over a required frequency range from 0.1 to 40 MHz. The MTs have to be balanced pair-wise within 0.1 dB and the geometry of windings has to be mechanically stabilized using e.g. epoxy resin. A choice of different epoxy types and their suitability for cryogenic operation was tested in LN₂.

METHODS AND RESULTS

For the heavy ion synchrotrons where bunches with the length of several meters revolve with a frequency of few MHz high impedance coupling of the BPM is advantageous because it delivers a larger signal strength. Since the signal strength decreases with increasing capacitance high impedance amplifiers are typically mounted directly on BPM vacuum feed-throughs. However, in the case of SIS100, due to the heat deposit raised by amplifier power losses, the amplifiers have to be installed outside the cryostat [3]. The length of the signal lead inside the vacuum vessel has to be about 2.5 m – on the one hand – to overcome space between the BPM and cryostat cable ports and – on the other hand – to keep the heat flow through all four signal leads below 0.5 W per single BPM. In addition, the expected radiation level in the neighborhood of BPM station can reach the level of some kGy per year, thus exceeding the maximal tolerable radiation dose for the head electronics by almost one order of magnitude. Therefore,

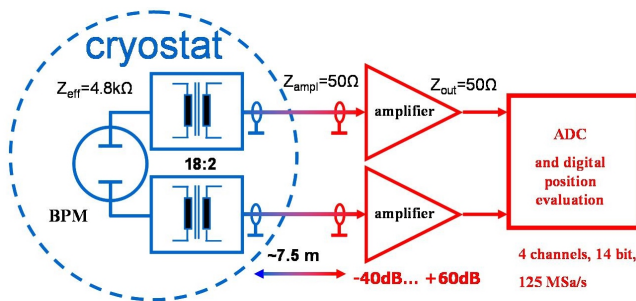


Figure 1: Schematic diagram of impedance matching by means of matching transformer.

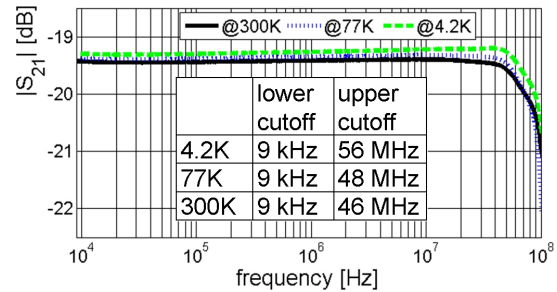


Figure 2: The transfer function of the optimized MT at different temperatures.

the cable lengths have to be extended by another five meters to move the amplifiers away from the beam pipe. For reflection free signal transport in such long signal lines an impedance matching to 50 Ω close to the BPM plates by a passive transformer is necessary [4], see Fig. 1. The realization described here has a winding ratio of $N_{pri}/N_{sec} = 18 : 2$ and is based on a toroidal core with external/internal radius and thickness of $r_e = 15 \text{ mm} / r_i = 10 \text{ mm}$, $h = 10.5 \text{ mm}$, respectively. The input impedance of the amplifier $Z_{ampl} = 50 \Omega$ is transformed proportionally to the square of the winding ratio $Z_{eff} = (N_{pri}/N_{sec})^2 \cdot Z_{ampl}$, yielding an effective impedance of about 4.8 kΩ. Because the voltage ratio for a transformer is given by $U_2/U_1 = N_2/N_1 = 18 : 2$ the signal strength U_2 is nine times smaller compared to the high impedance case. On the other hand, the thermal noise is lower compared to the high impedance termination due to the scaling of the noise voltage $U_{eff} \propto \sqrt{R}$. The influence of a transformer on the resulting BPM signal shape for a single bunch as well as for a train of bunches is discussed more precisely in [5].

The transmission function is the most important MT parameter and can be determined by a vector network analyzer by measurements of the scattering parameter S_{21} . For the shortest bunch length of 50 ns and revolution frequency in the order of one MHz a reasonable bandwidth of the transformers that is able to transmit the full signal shape and its full power spectrum is $\sim 0.1 \text{ MHz}$ to 40 MHz [3]. Since the transfer function can be extended toward the lower frequencies by using toroid materials with high relative permeability Vitroperm 500 F was chosen [6]. An advantage of this material is its high saturation induction $B_s = 1.2 \text{ T}$. This is extremely important with regard to the dynamic range of the signal amplitude of over 120 dB [3]. At best the transmission is very linear over the whole relevant frequency range exceeding significantly the required bandwidth. This can be seen in Fig. 2 where the frequency dependence of S_{21} measured at different temperatures is shown. The table in Fig. 2 summarizes the useful MT bandwidth (defined as the frequency range, in which the S_{21} variation is smaller than $\pm 0.1 \text{ dB}$). Since the bandwidth even grows with decreasing temperature the

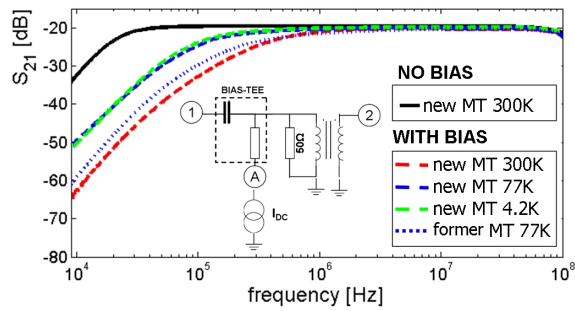


Figure 3: The transfer functions measured with and without DC bias at different temperatures, see text. Data for the dotted line are taken from [8].

new MT based on Vitroperm-500F core can be successfully used in the cryogenic environment. The high linearity of the MT transmission can be deteriorated, mostly at the lower frequencies, by core saturation that occurs for the highest expected BPM signal amplitudes. First investigations of the former MT type described in Ref. [8] (dimensions: $r_e = 8.6$ mm, $r_i = 5.9$ mm, $h = 7.4$ mm, winding ratio 18 : 3) had shown strong saturation effects ranging from 40 dB at 100 kHz down to 5 dB at 1 MHz, respectively. This exceeds the allowed value by almost two orders of magnitude [3]. To reduce the saturation influence on the transfer function, the optimized MT toroidal cores have a larger cross section and lower number of primary windings compared to the design from [8]. To simulate the core saturation the primary MT winding was biased with a DC current via a BIAS-TEE using the setup schematically shown in Fig. 3. The solid line in this figure presents the transmission function without DC bias and corresponds to that in Fig. 2. The additional low frequency limitation is caused by the high pass characteristics of the BIAS-TEE. The dashed lines show the transmission at a bias current of 450 mA which is equivalent to the highest expected signal amplitude of 1.8 kV [3]. Note, that the saturation effects at the low temperatures (77 K and 4.2 K) are much smaller than at room temperature due to the temperature dependency of the saturation polarization. This tendency, observed already for other nanocrystalline alloys [10], is advantageous when MTs are operated at cryogenic conditions. Moreover, optimized MT, with the larger toroid cross section, are by a factor of two less bias sensitive in comparison to the former used cores (dotted line).

Test of Transformer Encapsulation

Due to possible geometry changes during thermal cycling transformer windings have to be stabilized using e.g. epoxy resin. The choice of a proper epoxy type is an issue: material has to be suitable not only for insulation vacuum of about 10^{-7} mbar but also for cryogenic conditions. Particularly its linear thermal expansion has to be matched to the expansion of the MT toroid material. Otherwise either the epoxy or toroide may crack. At the lower temperatures, i.e. below 100 K, the commonly used *Temperature coefficient of thermal expansion* $\alpha \equiv (1/L)dL/dT$ becomes highly nonlinear and is usually substituted with

Table 1: Epoxy Resins Used in the Tests. Values of total thermal contraction $\Delta L/L$ are taken from [7].

Main constituent	Second constituents	$\Delta L/L$ [%] 395 to 4 K
Stycast 2850 FT	Catalyst 24 LV	1.2
Stycast 2850 KT	Catalyst 24 LV	–
Stycast 2850 GT	Catalyst 24 LV	0.42
Araldite CW 299-3	Araldite CW 299-1	1.06
Stycast 1266 A	Stycast 1266 B	1.15

the so called *total thermal contraction* $\Delta L/L$ that is integrated over a given temperature range [2]. Since the MT toroid is build out of nanocrystalline ribbon wound alternately with an insulating foil, a determination of its total thermal contraction can only be done by empiric comparison with epoxy materials of known total thermal contraction. The contraction of the epoxy resin can be controlled by a choice of material with proper contents of ceramic admixtures. Five epoxy resins with slightly different thermal contraction were tested, as listed in table 1. Great attention was put in the preparation of the samples. Epoxy constituents were mixed with a precision of 10^{-3} (0.1 g). An admixture of Antifoam 88 was used to reduce the surface tension and to remove air bubbles from epoxy material. In addition, the MT encapsulations (shown in fig 4) after filling with epoxy were kept 10 min. in a 0.1 mbar vacuum for outgasing. After that samples were stored in a temperature controlled oven as specified in the epoxy documentation.

For each epoxy type four samples were prepared and tested with LN_2 in a bath cryostat. The MTs were cooled down over 20 minutes. As shock cooling, would generate additional stress in the epoxy, the cooling time was prolonged by a connection of a semi-rigid cable extension with the length of about 20 cm to the N-type connector. MTs with this extension were slowly immersed into liquid nitrogen until the whole MT chassis was covered. In the next step samples were warmed up to the room temperature within 20 minutes in the temperature controlled oven. Ten such cycles were performed for all four samples of each epoxy type. All epoxy resins with total thermal contraction in the order exceeding 1% (Stycast 2850 FT, Araldite



Figure 4: Matching transformers non-encapsulated and encapsulated in epoxy (from left top to down bottom). The order is the same as in Table 1.

CW 299-3 and Stycast 1266 A/B) were affected by many cracks in the structure whereas the last was completely broken already after first cycle. On the contrary, Stycast 2850 KT and Stycast 2850 GT showed to be suitable for MT operation in cryogenic temperatures. Electrical features of MT measured after cryogenic test remain unchanged which proves that the toroids were not destroyed in cryogenic tests.

Since encapsulation of the transformers has to be suitable for the insulation vacuum of the cryostat measurements of the outgassing rate were performed by means of the accumulation method reported in [9]. For each epoxy resin 1 mm thick samples of $5 \times 10 \text{ cm}^2$ were prepared. Since measurements of outgassing rate are in progress (test of one sample takes 50 days) only results for Stycast 2850GT can be presented, see Fig. 5. The outgassing of epoxy is driven by two main processes: desorption from the surface and diffusion of the gases bounded in bulk material. At the beginning of the pumping process desorption is dominant. After about 10 hours of pumping the surface of the sample is more or less free of adsorbed gases and diffusion becomes dominant. Both outgass processes have more or less an exponential character with two different time constants: τ_1 and τ_2 . This is typical for plastic materials like epoxy [9]. Data points in Fig. 5 were fit by means of nonlinear least square method using a function: $f(x) = a \cdot \exp(-\frac{t}{\tau_1}) + b \cdot \exp(-\frac{t}{\tau_2})$, whereas the coefficients for a desorption and diffusions are $a = 5.37e - 7$, $\tau_1 = 4.55 \text{ h}$, $b = 9.5e - 9$, $\tau_2 = 114.9 \text{ h}$, respectively. Fluctuation of the outgassing rate that can be seen starting from about 40 hours of pumping are caused by day-night environment temperature changes of $\pm 2^\circ\text{C}$. After 100 hours of pumping one reaches the outgassing ratio of $3.6e-8 \text{ mbar} \cdot \text{l/s/cm}^2$ which is almost two orders of magnitude smaller than for non-machined Araldit-epoxy usually used in the cryogenic applications [11]. Since the area of epoxy used in MT encapsulation and exposed on the vacuum is only about 10 cm^2 one can state that contribution to overall outgassing rate of four MT installed to one BPM is negligibly small compared to e.g. contribution of super-insulation used in SIS100 cryostats. Constituents of the outgassing flux from the epoxy were analysed by a quadrupole mass spectrometer. Resulting mass spectrum is shown in Fig. 6. The spectrum is dominated to more than 95% by the products of thermolized water and water va-

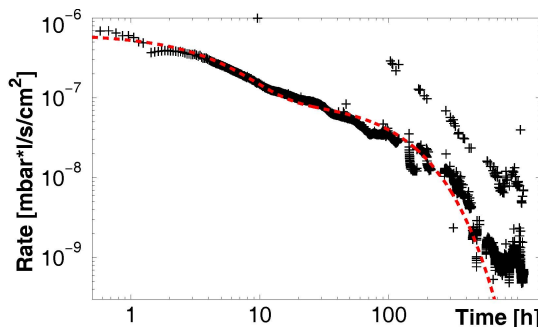


Figure 5: Outgassing rate for Stycast 2850 GT, see text.

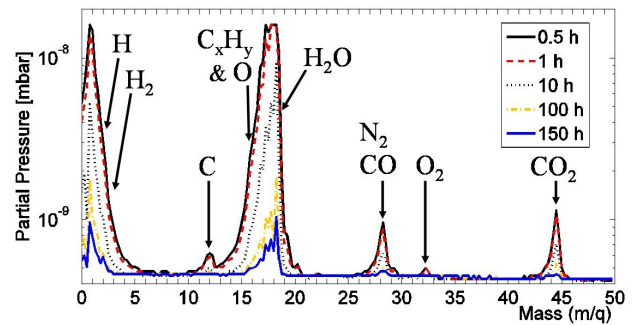


Figure 6: Mass spectrum of the constituents of the outgassing flux for Stycast 2850 GT, see text.

por. An yield of hydro-carbon gases C_xH_y that should appear as a peak at mass of 16 and which should significantly contribute to carbon peak at mass of 12 is not observed which is an evidence that the tested epoxy is not contaminated with the organic solvents or oils. Therefore, Stycast 2850 GT can be assumed suitable for insulation vacuum.

CONCLUSIONS AND PERSPECTIVES

It was shown that the optimized matching transformers are able to transmit BPM signals in the required frequency range. To minimize the offset of the BPM position determination the MTs have to be pairwise balanced within $\pm 0,1 \text{ dB}$. Moreover, the geometry of windings has to be stabilized using e.g. Stycast 2850 GT that is suitable at the insulation vacuum and its total thermal contraction match the one of toroid material. For a complete prove of the cryogenic suitability of the encapsulation further tests in LHe are required.

ACKNOWLEDGMENT

Authors owe thanks Dr. S. Wilfert and Dr. H. Kollmus from GSI UHV group for valuable help in interpretation of the outgassing results.

REFERENCES

- [1] "FAIR Technical Design Report SIS100", GSI Darmstadt, Germany (2008) p.335
- [2] J. W. Ekin, "Experimental Techniques for Low-Temperature Measurements", ISBN: 978-0-19-857054-7 (2006) p.233
- [3] P. Kowina et al., *Proc. EPAC'06*, Edinburgh (2006) p.1022
- [4] J. Schölles, et al., *Proc. DIPAC'03*, Mainz (2003)
- [5] P. Forck et al., *CAS "Beam Diagnostics"*, Dourdan (2008)
- [6] <http://www.vacuumschmelze.de>.
- [7] G. Ventura and L. Risegari, "The art of cryogenic", ISBN:978-0-08-044479-6 (2008) p.72, CA. Swenson, *Rev Sci Instrum* (1997;68), p1312.
- [8] P. Kowina, et al., GSI Scientific Report (2007)
- [9] K. J. Wutz, "Handbuch Vacuumtechnik", ISBN:3-528-64884-8
- [10] R. Grössinger, et al. "Advanced Engineering Materials", ISSN: 1527-2648 (2008) p.285
- [11] A. K. Gupta et al. *Vacuum*, Vol. 27:2 (1976) p.61